# Elastohydrodynamic Study of Deformable Blade-Organic Photoconductor Conjunction

***Wael Salalha & Doron Avramov, Hewlett-Packard Indigo division - Rehovot, Israel 76101***


## Abstract

*In Liquid electro photography (LEP), deformable blades are used to remove ink residuals and liquid from the Organic Photoconductor (OPC) drum. The thin layer remaining after the blade can produce undesirable chemical residuals on its surface. When bombarded by ions at the charging station, this layer can oxidize and affect the OPC's electrical properties. In this work we investigate the blade-OPC drum conjunction under fully flooded inlet and outlet conditions; a theoretical model incorporating elastohydrodynamic (EHD) considerations was developed where a deformable blade is deflected by a moving surface (OPC). Unlike typical EHD problems which are widely discussed in the literature, our case consists of a contact line which causes singularity problem in the analysis. This singularity is due to the blade's sharp corner edge prior to its deformation. In order to overcome this singularity, we first solved the elastic-static deformation of the tip using finite element simulation (COMSOL) and combined hydrodynamics considerations afterwards. Experimental results were found with good agreement to our calculations. We found that for a 2 [mm] width blade (1.2 [mm] deflection), the film thickness remaining after the OPC surface wiping is about 25 [nm]. The contact nip length is 12 [μm], where the maximum conjunction pressure was found to be 4 [MPa] and 1.8 [MPa] under static and elastohydrodynamic conditions, respectively.*


## Introduction

Flexible blades are most widely used for fluid removal out of moving surfaces in printing, coating, chemical process and other applications. In typical digital printing machines a deformable flexible blades is used to remove remaining oil from the Organic Photoconductor drum (OPC drum) after a cleaning station and before a charging station as shown in Fig. 1. A schematic illustration of a cleaning station system is shown in Fig. 2, a wetting roller (marked as 1 in Fig. 2a) raises the oil to the surface, a sponge roller (2) removes the fluid from the surface and the blade (3) cleans the remaining oil. The film thickness that was removed by wiping the surface is of an order of ~10 [μm], while the remaining film thickness is of the order of 10s of nanometers. If above certain thickness (~100 [nm]), the film which is left after the blade can produce undesirable coating layer on the OPC surface when bombarded by ions at the charging station [1]. In addition and under specific conditions, stuck particles which are between blade tip and OPC can cause mechanical scratches. Thus, there is great interest in understanding the interaction between the blade tip and the OPC drum. In this work we have modeled the blade OPC drum conjunction, where a deformable blade deflects against a moving surface under flooded conditions. This problem can be considered as a line contact elastohydrodynamic (EHD) problem. Elastohydrodynamic lubrication (EHL) is typically used when the pressure is high and the surfaces are elastically deformed and having relative velocities [2]. Hamrock and co-workers investigate EHL for over 30 years [3-6]. Their models include surface characterization, viscous effects and elastohydrodynamic lubrication [3,4,5]. Dowson reviewed the development and the understanding of fluid film lubrication in a deep review of EHL, which includes line and point contacts [2]. In another paper he reviewed the development of the thinning film in lubrication theory and included the phenomenon occurred at very thin films [6]. Hu and Granick reviewed the effects of nano-rheology on tribology [7]. Skotheim and Mahadevan considered the coupling between fluid flow and elastic deformation in confined geometry [8]. Flow between a rigid cavity and a flexible wall was demonstrated by Yin and Kumar [9]. The above cited studies considered solutions for two rollers or roller and a flat surface in contact situations, such as bearings, gears or seals with defined radiuses at the contact points.

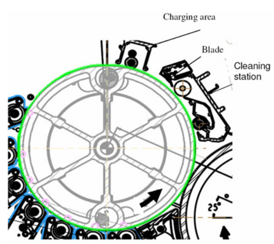


***Figure 1:*** *general view of a photoconductor drum (OPC) and the cleaning station*

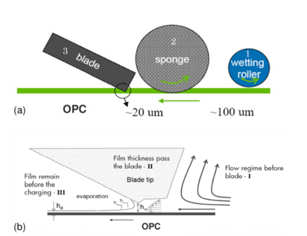


***Figure 2:*** *(a) Schematic illustration of the cleaning station, (b) A focus on the blade tip OPC conjunction.*

Unlike typical EHL problems mentioned above which were widely discussed in the literature, our case consists of a contact line which causes a singularity problem in the analysis. This singularity is due to the blade's sharp corner edge prior to its deformation (see Fig. 2a). For the best of our knowledge, no work has dealt with a configuration which consists of a sharp corner in contact with a moving surface under hydrodynamic conditions as illustrated in Fig. 2b. Prior to the conjunction, one can consider the flow regime as a corner flow between a plane at rest (the blade plane) and scraped plane parallel to itself (OPC drum) [10,11]. In order to have an appropriate analytical model of the second region (II), elastohydrodynamic considerations must be taken into account. This model should predict the film thickness under the flexible blade as well as pressure developed at this conjunction. The third region (III) which determines the fluid layer between the conjunction and the charging area can be described as withdrawn problem under constant flow in the inlet channel. In this paper we dealt mainly on region II.

## Analytical and numerical approaches

The main aim of this study is to analytically and experimentally determine the film thicknesses left after the blade-OPC drum conjunction. Another goal is to find the forces between the blade tip and the OPC drum. To achieve these goals and overcome singularity issues, we first solved the **elastic static deformation** of the tip and combine **hydrodynamics considerations** afterword. Once we find the elastic deformation of the blade tip, we assume minor changes occur in the blade deflection and then we add the elastohydrodynamics considerations.

## Elastic static deformation

First, we found numerically the contact length (nip) and pressure distribution on blade's tip consisting of a sharp corner prior to the deformation. To this end, COMSOL software was employed for a numerical simulation of this problem [12]. Consider a long polyurethane blade resting on a flat polycarbonate (OPC drum) foundation, where both structures are elastic. The OPC drum is subject to constant displacement perpendicular to its surface in the z direction. To overcome the blade tip singularity problem, we assumed a tip radius of 0.5 [µm] which is small enough to the expected deformed area and refined the numerical mesh at this region. Fig. 3a shows a numerical result of a deflected blade with typical dimensions of width=2 [mm] and length=30 [mm], where the displacement of the OPC surface is 1.2 [mm] in the z direction. Fig. 3b is a magnification of the deformed blade tip, where the nip length was found to be 12 [µm]. In Fig. 3c we see the pressure distribution on the tip edge for the same example. We note that a high pressure and an asymmetrically distributed around the blade tip were found as expected. Results of the forces and lengths are summarized in table 1.

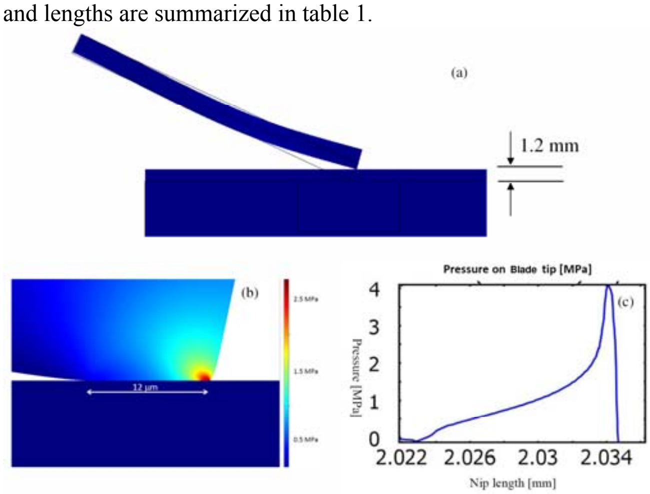


***Figure 3:*** *(a) COMSOL result of the blade and OPC system after loading by displacement the OPC, (b) Von Misses stresses of the blade tip, (c) Pressure distribution on blade's tip in MPa as a function of nip length.*

## Elastic static deformation – Experiment

Several experiments were conducted in order to validate these numerical results. In order to find the total force acting on the blade's tip we used direct measurements under deflection. In addition a PDMS (Sylgard 184 Silicon) curing method was also used to find the nip length of the blade. These results (summarized in Table 1) were found to be in good agreement with our calculations. The measured forces showed some deviations from calculations, which can be related to friction and inaccuracy of the experimental setup. Fig. 4a illustrates the molded PDMS under the deformed blade edge, and Fig. 4b is an optical microscope image of the nip length after peeling the blade from the surface.

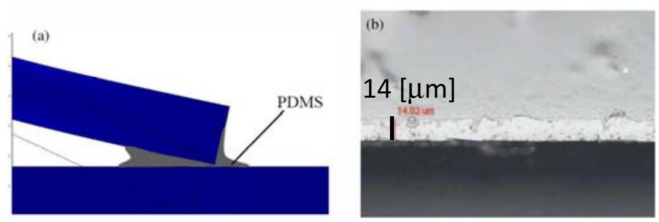


***Figure 4:*** *(a) Illustration of the molded PDMS under the deformed blade tip, (b) an optical microscope picture of the nip length after peeling the blade from surface.*

**Table 1: Force and nip lengths of 2 [mm] and 3 [mm] blade widths**

| | 2 [mm] blade with 1.2 [mm] deflection | 3 [mm] blade with 1.2 [mm] deflection |
|---|---|---|
| Total Normal Force between blade and OPC (COMSOL); measured | (12 [N/m])<br>18 [N/m] | (55 [N/m])<br>75 [N/m] |
| Nip length of blade<br>(COMSOL); measured | (12 [µm])<br>14 [µm] | (45 [µm])<br>50 [µm] |
| The minimum gap calculated under blade tip | 25 [nm] | 45 [nm] |

## Elastohydrodynamic solution

We used the EHD interaction to find the liquid film thickness under the blade's tip. The OPC drum deflects the blade which causes a local deformation of the blade tip (a static elastic deformation). Then, movement of the OPC drum under fully flooded conditions inverts the problem from static into elastohydrodynamic. Typically, in order to include the elastic deformations in the elastohydrodynamic interaction, the Reynold's equation for the fluid is coupled to elastic modulation and then a numerical method is used for solving a non linear ordinary differential equation (ODE). We assume that the hydrodynamic solution will not change the tip shape nor the total forces acting on the blade.

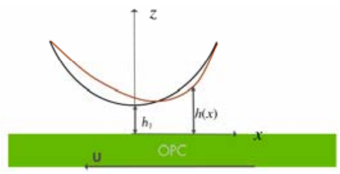


***Figure 5**: a schematic illustration of the deformable elastic surface before and after OPC surface movement.*

A parabolic function is used to describe the shape of the deformable surface before the hydrodynamic consideration as shown in Fig. 5. The distance between the lowest point of this function and the OPC surface is denoted $h_1$. Thus, the distance can be expressed by

$$h(x) = h_1 + \frac{x^2}{R} + D(x)\,, \tag{1}$$

Where $R$ is the radius of curvature of the upper surface, and $D(x)$ is the gap change due to the elastic deformation. Using Coyle's assumption that local deformation is propositional to the local pressure of the liquid flow we obtain an expression for $D(x)$ [13].

$$D(x) = \frac{P(x)\cdot L}{E}\,, \tag{2}$$

where $L$ is defined as the effective length of the deformable part, $E$ is the effective elastic modulus. The liquid flow under the deformed part is governed by Reynold's equation,

$$\frac{\partial}{\partial x}\left(\frac{h^3}{\eta}\frac{\partial P}{\partial x} + 6\cdot U\cdot h\right) = 0\,, \tag{3}$$

where $P$ is the pressure, $\eta$ is the liquid viscosity and $U$ is the tangential speed of the moving surface. After dimensional analysis while using length scale $\sqrt{h_1\cdot R}$, velocity scale $U$ and a pressure scale $\frac{\sqrt{R}\cdot\eta\cdot U}{h_1^{3/2}}$, we obtained the following set of equations:

$$\frac{\partial}{\partial \hat{x}}\left(\hat{h}^3\frac{\partial \hat{P}}{\partial \hat{x}} + 6\cdot\hat{h}\right) = 0\,, \tag{4}$$

$$\hat{h} = sign(h_1) + \hat{x}^2 + Ne\cdot\hat{P}\,, \tag{5}$$

where $Ne = \frac{\sqrt{R}\cdot\eta\cdot U\cdot L}{h_1^{2.5}\cdot E}$

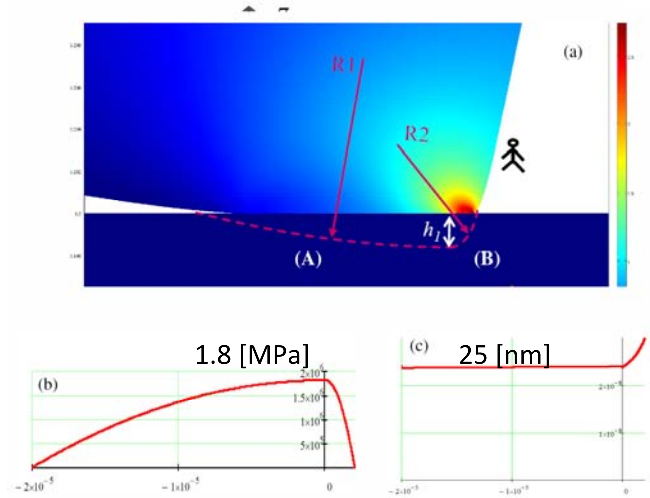


***Figure 6:** (a) Illustration of the two regions, A and B, (b) typical result of the pressure [Pa] distribution under the tip of the blade, (c) typical result of the film shape under the deformed blade tip after numerical calculation [m].*

Naturally, these well known equations are valid for symmetric and predefined parabolic shape surfaces before deformation only. However, in our problem the blade's tip is asymmetrically located relative to the OPC surface. In order to overcome this complexity, we divided the blade's tip conjunction into two regions. The first region (A) is considered from the outlet up to the maximum pressure point, where region (B) extends from the maximum pressure point to the inlet as shown in Fig. 6a. The connection point between these two regions is defined by pressure reaches maximum and equal pressure derivative. Examining Fig. 6a, we can estimate the radii of each region. $h_1$ can be defined by finding the intersection between these two radiuses where $L$ is calculated as $L = \frac{E\cdot h_1}{P_{\max}}$. Finally, we iteratively solved equations (4,5) by changing the boundary conditions of the nip length and having the calculated total force as a constrain. An example of the pressure distribution under the tip is shown in Fig. 6b. It is clear that the maximum pressure obtained is smaller relative to the static solution due to larger nip under flooded situation. A typical film thickness under the deformed blade tip is shown in Fig. 6c. The results of the numerical solution for different geometrical parameters are summarized in Table 1. As shown, the film thickness based on the EHD model for different geometrical parameters were found to be 25 [nm] and 45 [nm] for 2 [mm] and 3 [mm] blade widths respectively. Note: despite of the small film thickness obtained, the non-slip boundary condition assumption is still valid [14].

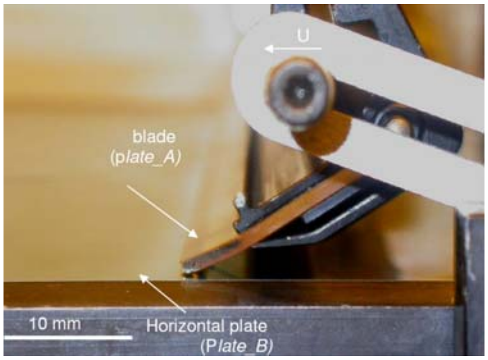


***Figure 7:*** *Experimental setup.*

## Elastohydrodynamic - Experiment

In order to validate our results, we injected nanoparticles dispersion with different sizes prior to the blade in experimental setup that is shown in Fig. 7. Fig. 8a and 8b show the particles image and sizes distribution. The experimental setup consists of a blade (plate_A) which rests on flat horizontal surface (plate_B) simulating the OPC drum. Plate_A can move with a constant velocity in the range of $V = 5-20\,[cm/\sec]$. High resolution SEM image of OPC surface (Fig. 8c) shows that nanoparticles above 30 [nm] do not pass the blade (for a 2 [mm] width blade). In another test, using the same experimental setup, we used a high viscosity fluid and measured its thickness profile after curing. The expected results were in the order of ~200 [nm] which can be measured optically. We used varnish #7963 purchased from Nicoat (μ=75 [mPa·s]) which was cured using a UV lamp (λ=350 [nm]). The film thickness measurements were carried out by a spectrophotometer (Varian Â®Cary5000 UV-visible-NIR) which can measure the intensity of light reflected from a thin film over a range of wavelengths. The thickness of the film was calculated from the spectral interference pattern obtained by the way analogous to the one described by Xiong et al. [15]. The results are summarized in Table 2. They show a good agreement between experimental and calculated results.

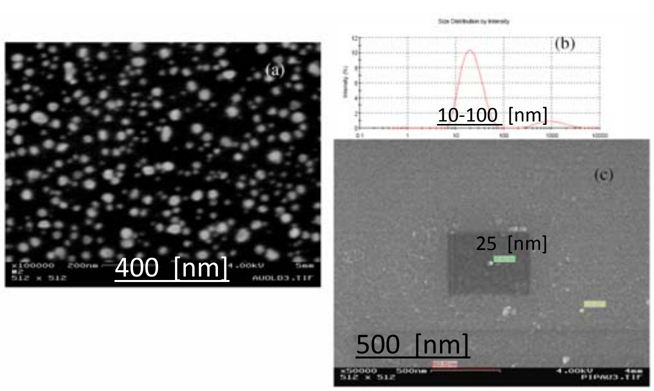


***Figure 8:*** *(a) High resolution scanning electron microscope (HRSEM) picture of the injected gold nanoparticles, (b) graph of size distribution of the nanoparticles, (c) High resolution SEM picture of the surface after wiping the nanoparticles by the blade.*

**Table 2: Film thickness remaining after a 2 [mm] blade width.**

| Film thickness [nm] Varnish (#7963) | Blade Velocity | |
|---|---|---|
| | 0.12 [m/s] | 0.2 [m/s] |
| Measured thickness | 250 [nm] | 465 [nm] |
| Calculated thickness | 240 [nm] | 420 [nm] |

## Summary

In this paper we developed numerical and experimental methods for blade OPC conjunction under hydrodynamic considerations. We find that the film thickness that passed the blade was of the order of several tenths of nanometers. A good agreement between experimental and numerical results was found.

**Acknowledgments:** thanks for Prof. Eyal Zussman and Dr. Slava Resnik from the Technion and for Dr. Boaz Tagansky and Dr. Yoram Sorek from HP, Indigo for their good discussions and help.

## References

1. S. Chang, O. Gila, T. Anthony, P. Matheson, and M. Lee, Measurements of PIP oil layer thickness and evaporation rate, HP Labs (internal document) (2007).
2. D. Dowson, Elasohydrodynamic and micro-elastohydrodynamic lubrication, Wear 190, 125-138 (1995).
3. B. J. Hamrock, Fundamentals of fluid film lubrication, McGraw-Hill, Inc. (1994).
4. B. J. Hamrock, and B. O. Jacobson, Elastohydrodynamic lubrication of line contacts, ASLE/ASME lubrication conference in Hartford, 18-20 (1983).
5. Elsharkawy, and B. J. Hamrock, Elastohydrodynamic lubrication of elastomeric-coated surface in line contact, Journal of Engineering Tribology 18, 209-221 (1995).
6. D. Dowson, Development in lubrication – the thinning film, J. Phys. D: Appl. Phys. 25, A334-A339 (1992).
7. Y.-Z. Hu and S. Granick, Microscopic study of thin film lubrication and its contributions to macroscopic tribology, Tribology Letters 5, 81-88 (1998).
8. J. M. Skotheim, and L. Mahadevan, Soft Lubrication, Physical review letters 92, 245509-1-4 (2004).
9. X. Yin, and S. Kumar, Lubrication flow between a cavity and flexible wall, Physics of fluids 17, 063101-1-13(2005).
10. H. K. Moffatt, "Viscous and resistive eddies near a sharp corner", Journal of Fluid Mechanics 18, 1 (1964).
11. J. Riedler and W. Schender, "Viscous flow in corner regions with a moving wall and leakage of fluid," Acta Mechanica, 48, 95-102 (1983).
12. COMSOL 3.4, www.comsol.com.
13. D. J. Coyle, "Forward roll coating with deformable rolls: A simple one-dimensional elastohydrodynamic model," Chem. Eng. Sci. 43, 2673 (1998).
14. J. Koplik and J. R. Banavar, "Continuum deduction from molecular hydrodynamics," Annu. Rev. Fluid Mech. 27, 267 (1995).
15. D. Xiong, H. J. Zhang, and D. X. Zhang, "In-situ thickness measurement system for porous alumina film based on AFM and spectrometer", 4th International Symposium on Instrumentation Science and Technology (ISIST' 2006) 48, 1073 (2006).

## Author Biography

*Wael Salalha finished his Ph.D. degree and postdoctorate in mechanical engineering at the Technion, Israel Institute of Technology in (2005) and (2007), respectively. His research fields were on Nano/Micro-Fluidics, Nanotechnology and Electrospinning of functionalized polymeric nanofibers. He currently is a physicist at Hewlett Packard, Indigo Division.*

*Doron Avramov has M.Sc. in mechanical engineering focusing on analysis of small scale inhomogeneities in turbulent flow using PIV methods. He currently serves as a team manager leading the photoconductor research at Hewlett Packard, Indigo Division.*